Reduction of vortex-induced vibrations by locally resonant metamaterials

F. Alves Pires [1,3], **H. Denayer** [1,3], **E. Deckers** [2,3], **C. Claeys** [1,3], **W. Desmet** [1,3]
[1] KU Leuven, Department of Mechanical Engineering,
Celestijnenlaan 300, B-3001, Heverlee, Belgium

[2] KU Leuven, Diepenbeek Campus, Mechanical Engineering Technology TC,
Wetenschapspark 27, 3590 Diepenbeek, Belgium

[3] DMMS Lab, Flanders Make, Belgium

Abstract
Flow-induced noise and vibrations are present in a variety of sectors such as automotive and aerospace, where reducing the noise and vibration harshness behavior has become a challenging task. Due to the current ecological trends towards the use of lightweight designs, novel low mass and compact solutions are sought to improve the dynamic behavior of such designs. Locally resonant metamaterials have recently come to the fore as potential candidates due to their superior noise and vibration reduction performance as a result of their ability to create stop band behavior, i.e. frequency zones of strong vibration and/or noise attenuation. This paper experimentally investigates the potential of using locally resonant metamaterials to improve the flow-induced vibrations phenomena under the influence of vortex-shedding.

1 Introduction

Flow-induced induced cabin noise has become a major topic for a variety of high speed vehicles. In an aircraft, for example, the pressure fluctuations of the turbulent flow generated over its fuselage can produce high levels of noise inside the cabin during cruise conditions, directly affecting the comfort of passengers [1]. Comparatively, in the automotive sector, the vibrations occurring on the underbody of a moving car are created by an unsteady turbulent flow, causing noise to be radiated into the cabin.

A wide number of these engineering problems are related with the flow around bluff bodies. If the bluff object is a circular cylinder, alternating vortices in a von Karman vortex street pattern are produced and shed as a result of boundary layer roll-up. These vortices continue to grow under continuous injection of circulation from the cylinder shear layers until they become strong enough to draw the shear layers across the wake [2]. The vortices stop increasing their strength and shed away from the cylinder as the vortices with an opposite sign in sufficient concentration stops further supply of circulation to the forming vortex [3]. This phenomenon is often referred to as vortex-shedding. The frequency of vortex-shedding i.e. $f_s = St\ U_\infty/D_c$, has been investigated over a broad range of $Re = U_\infty D/\nu$ from approximately 50 to 10^6 and even higher [4], where U_∞ is the free stream velocity, St the Strouhal number, ν the fluid kinematic viscosity, D_c the bluff cylinder diameter and D the duct diameter.

In fact, different solution techniques to reduce flow-induced noise and vibrations have been investigated and developed [5, 6, 7, 8, 9]. In the work of [5], for instance, several passive techniques are investigated and applied to an aircraft fuselage such as the addition of mass, damping and skin stiffness. In [8], an active control strategy is applied to a plate under flow excitation. Nevertheless, many of these countermeasures can be bulky and heavy and/or may not perform well in low frequencies [10]. For that reason, novel low volume and low mass countermeasures are required in order to tackle the challenges of not only achieving a good Noise, Vibration and Harshness (NVH) performance but also ensuring a lightweight design.

Recently, locally resonant metamaterials (LRMs) have attracted the attention and proven to hold great potential to combine a lightweight design and good NVH behavior in desired frequency regions, referred to as stop bands (SB). These are known as frequency zones where there is no free wave propagation [11] and can be achieved by adding resonant additions to a host structure on a subwavelength scale [12] due to a Fano-type interference [13, 14]. These zones of pronounced wave attenuation can be predicted by making use of dispersion diagrams, which can be calculated by a unit cell (UC) modeling approach utilizing the finite element (FE) method in combination with the Bloch-Floquet theorem [15, 16].

The present work aims to investigate the potential of LRMs to mitigate the flow-induced vibrations of a flat plate due to impinging vortices, originating from the vortex street in the wake of a cylindrical rod. A qualitative study is performed by means of Computational Fluid Dynamics (CFD) simulations in order to have an indication of the vortex-shedding evolution and how the formed von Karman street can interact with the plate. Experimentally, the vibrations of the bare plate under vortex excitation is compared with the structure's response for a grazing flow excitation. A realizable metamaterial design is then proposed and the flat plate treated. The experiments are repeated and the metamaterial performance to reduce the vortex-induced vibrations of the plate is assessed.

The paper is organized as follows. Section 2 introduces the host structure as well as the metamaterial design to achieve stop band behavior used in the investigation. It also shows the qualitative approach by CFD to have a first indication of how the vortex-shedding can interact with the host. Section 3 shows the experimental results of the vortex-induced vibrations of the metamaterial plate. Lastly, Section 4 summarizes the main findings of this paper.

2 Methodology

This section presents the host structure and the modeling techniques used to tackle the vortex-shedding problem.

2.1 Host Structure

With the aim of investigating the potential of LRMs to reduce vortex-induced vibrations, a steel flat plate with dimensions 150 x 200 x 0.5 mm is used as a host structure. This combination of material and dimensions of the system is chosen to have a flexible structure with pronounced modal behavior at the low-frequency range below 1000 Hz. The material properties of the host structure are shown in Table 1. They are obtained via modal analysis and model updating procedures from a rectangular panel of dimensions 350 x 451 x 0.5 mm, which is a cut-out of the same panel that the host structure is manufactured.

As illustrated in Figure 1, the considered host structure is placed on a duct section of a small wind tunnel with cross-sectional dimensions 150 x 75 mm, sufficiently distant from a rootsblower so that a fully developed flow can be achieved [17], and with a bluff cylinder of diameter D_c placed upstream to create a von Karman street.

A metal frame is used to attach the flat plate to the duct section by means of bolts. The plate is glued to the frame so that the plate can be assumed clamped along its boundaries. Given these conditions, the plate is then assembled flush as a side wall of the duct.

Table 1: Material properties of the steel plate.

Young's Modulus	Density	Poisson's Ratio	Structural Damping
233.1 GPa	7766.9 kg/m^3	0.27	0.2%

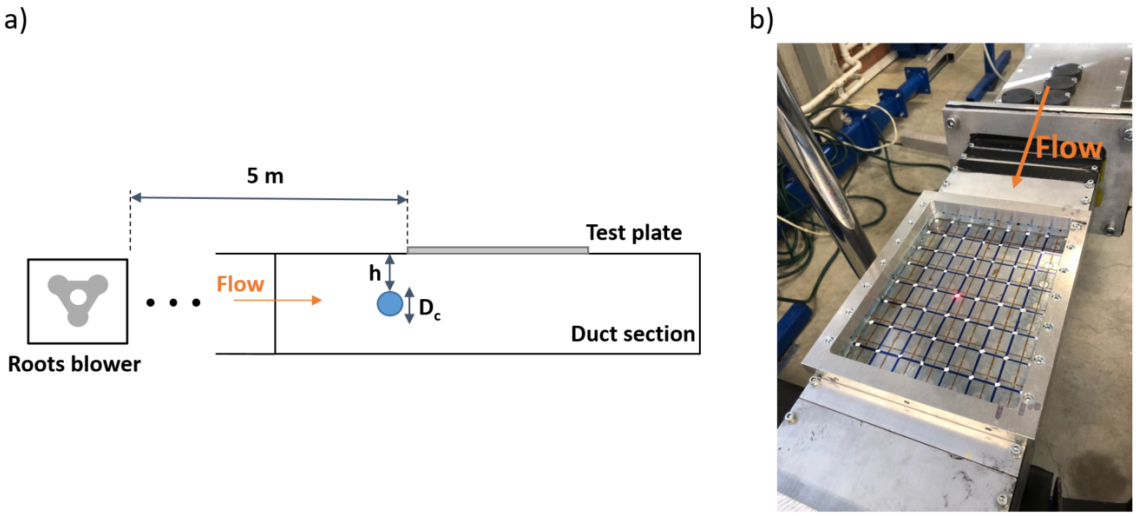

Figure 1: a) Schematic overview of the experimental fluid domain setup b) Steel flat plate attached to the duct section.

2.2 Unit cell modeling and metamaterial design

The typical periodic arrangement of resonant metamaterials is often studied by using unit cell modeling. This modeling technique is carried out by applying Bloch-Floquet periodic boundary conditions together with the finite element method (FEM), which leads to dispersion diagrams. The present work assesses the wave propagation of undamped infinite periodic structures from the calculation of the dispersion curves for an undamped unit cell, considering an irreducible Brillouin contour (IBC). For more information about the formulation behind this modeling technique, the reader is kindly referred to [11, 18, 19].

With the goal of designing a metamaterial solution, firstly, the dynamic behavior of the structure of interest needs to be obtained. With that in mind, the plate shown in Figure 1 is excited by an impact hammer of type PCB 086C03 without the presence of the flow. Its response is measured at 72 points by using a Scanning Laser Doppler Vibrometer (SLDV). Figure 2 illustrates the Root Mean Square (RMS) velocity response per unit force excitation of the plate. A metamaterial solution is then designed targeting a frequency region, namely, around 600 Hz, as the structure possesses pronounced dynamic behavior and the highest peak amplitude is measured within this frequency range, indicated by the red circle.

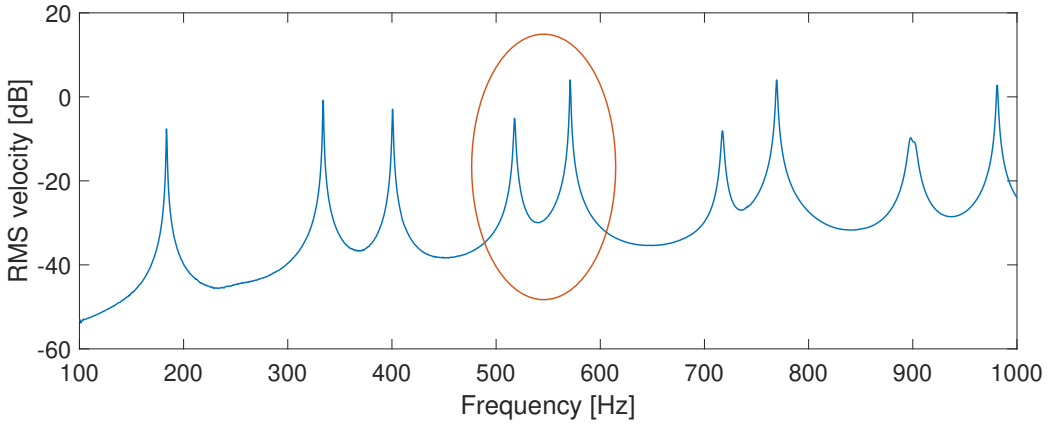

Figure 2: RMS velocity response of the clamped plate excited by an impact hammer. dB_{ref} = 1 (m/s)/N.

Figure 3 illustrates the proposed resonator design and an example of a realized resonator. A similar design is used in [20]. The design approach also takes into account the footprint of the realizable resonant additions, in which small footprints can lead to wider stop bands [21].

The resonant structures are added in a rectangular pattern with a spacing of 21 x 25 mm to the steel plate in order to be on a subwavelength scale at 600 Hz and achieve the desired stop band behavior. A total of 56 resonators are added to the host structure. The resonators add 29% of mass w.r.t the mass of the host structure. All resonators are made of polymethyl methacrylate (PMMA) and are 4 mm thick. The material properties of the PMMA are shown in Table 2.

To be able to compare, in a later stage, the metamaterial reduction performance with a classical solution e.g. mass treatment, a non-resonant mass block is also designed with the same footprint as the resonant additions to keep the same local added stiffness by the additions. Figure 3 illustrates the proposed design of a non-resonant structure and an example of this realized PMMA non-resonant addition with a similar percentage of added mass as the designed/realized resonators, namely, 28%. The difference in percentage of added mass between the realized resonant and non-resonant additions is due to manufacturing imprecision.

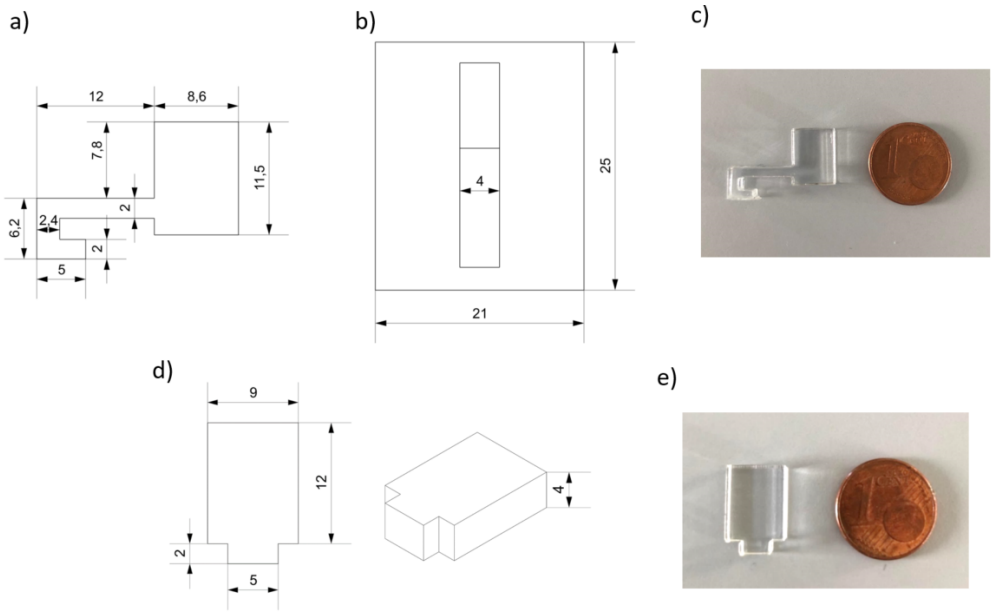

Figure 3: Illustration of the a) resonator design b) UC with resonator c) realized resonator d) non-resonant structure design and e) realized non-resonant structure.

Table 2: Material properties of PMMA [20].

Young's Modulus	Density	Poisson's Ratio	Structural Damping
4850 MPa	1188.38 kg/m^3	0.31	5%

The predicted stop band of the metamaterial design is illustrated in Figure 4. The different curves in the dispersion diagrams are distinguished according to the ratio of out-of-plane versus in-plane motion of the host structure. This analysis shows that a stop band for bending waves, identified by their out-of-plane motion, is created from 583.2 Hz to 634.9 Hz.

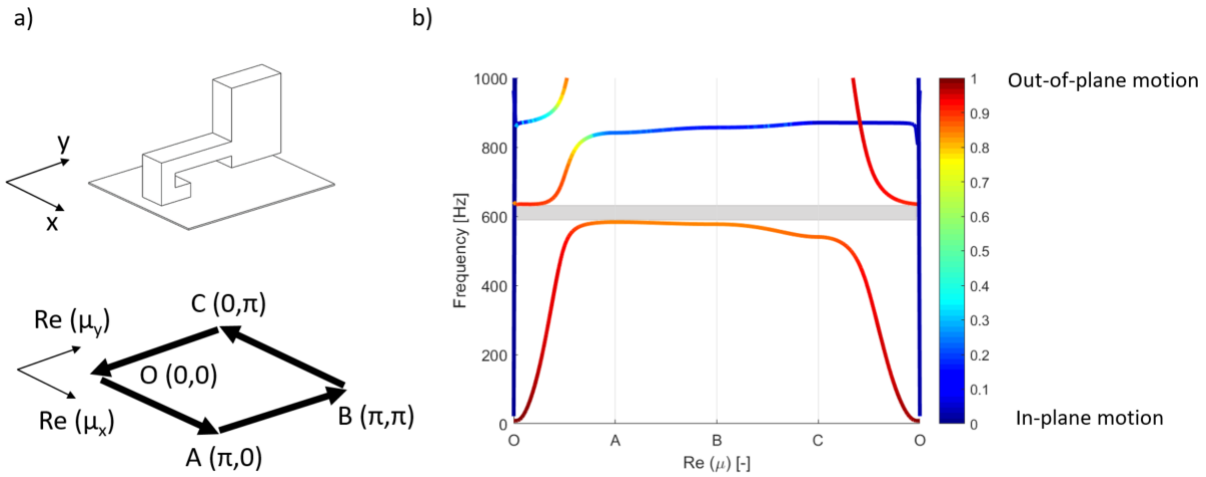

Figure 4: Representation of the a) Irreducible Brillouin contour with a sketch of the respective wave space b) Dispersion diagram in which the gray shaded area represents the predicted stop band. The color bar represents the ratio according to the out-of-plane and in-plane motion of the waves.

2.3 Vortex-shedding indication

The von Karman street is known as a tonal phenomenon generated when, for example, an unsteady turbulent flow in a duct finds a bluff object. If the forming vortices propagating at a certain frequency f_s come across an elastic structure e.g. flat plate, due to coupling effects of fluid-structure interaction, the structure can absorb part of the energy coming from the vortex-shedding, which can lead to an increase in the amplitude of structural modes near the vortex-shedding frequency [3] e.g. when compared with a grazing flow past a flat plate [22].

In order to have an indication of the vortex-shedding under the conditions shown in Figure 1 and its interaction with the structure of interest, targeting a frequency of f_s = 600 Hz, two dimensional URANS simulations are performed using Simcenter STAR-CCM+. For these simulations, the κ - ω model is used as this model works well for internal flows and gives good predictions near walls. A simplified 2D duct section with dimensions 2 m x 75 mm is then utilized in the analyses. It is considered that a flow of air with kinematic viscosity ν = 1.45 x 10^{-5} m^2/s and average speed U_∞ = 19 m/s, corresponding to a Reynolds number Re = 6.5 x 10^6 and Mach number M = 0.05, enters the domain from the left in turbulence conditions. From a fluid dynamics point of view, the bluff cylinder, the top and bottom walls are treated with non-slip boundary conditions whereas the outlet is considered as a pressure outlet.

The combination of the chosen frequency, flow speed as well as Strouhal number, i.e. St = 0.2 [23], results in D_c = 6 mm. Figure 5 illustrates the mesh for the duct containing the bluff object with diameter 6 mm positioned in the center of the duct to generate a vortex-shedding with frequency 600 Hz; the top and bottom walls as well as the cylinder are meshed with a boundary layer whose spacing resolution is based on the values of the y^+ smaller than 1 [17]. This parameter is a non-dimensional distance from a wall and it is often used to describe the height of the first grid element next to a wall in CFD simulations. The mesh is built up very fine close to the cylinder so that the wake of the vortex-shedding can be better depicted whereas in the regions before and after the cylinder towards the inlet and outlet, respectively, the mesh is built coarser in order to keep the computational cost affordable with an acceptable mesh convergence.

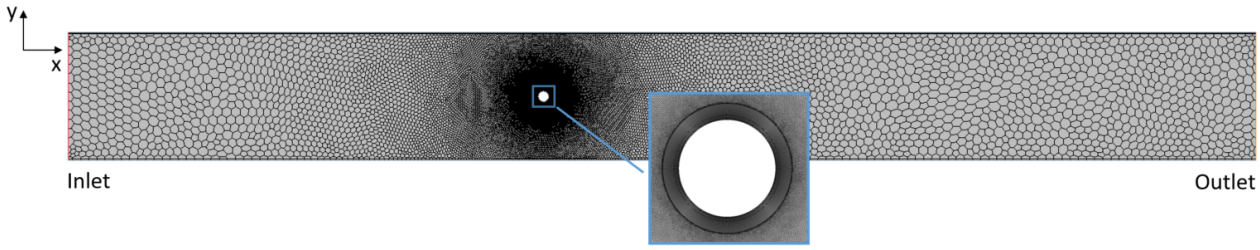

Figure 5: Sketch of the computational fluid mesh for a vortex-shedding prediction.

Two test cases are then performed by varying the ratio h/D_c i.e. relationship between the distance of the bluff object w.r.t. the flat plate and the bluff body's diameter, as in Figure 1 a), to have an indication of how close to the wall i.e. flat plate, the bluff cylinder can be placed so that the vortex-shedding can interact with the surface of interest. The chosen ratios are: (i) h/D_c = 6.75, this corresponds to adding the bluff object at the center of the duct and (ii) h/D_c = 1.0. It is taken into account that a h/$D_c \leqslant 0.3$ may lead to a cessation of the von Karman street, as indicated by [24]. Hence, ratios smaller than 1 are avoided in this work.

The time-step used for each simulation is 1 x 10^{-5} s. Moreover, they are run for a total time of 0.1 s. The convergence of the results are done via the CFD convergence criterion based on the residuals values e.g. values smaller than 1 x 10^{-6}, with an acceptable computational cost. Figure 6 illustrates the vortex-shedding over the cylinder for the considered conditions, in terms of vorticity. The analyses indicate that a von Karman street is indeed achievable in the considered conditions, and show that for smaller ratios h/D_c e.g. bluff cylinder placed closer to the boundary, a greater interaction between the vortex-shedding and the wall takes place i.e. it is possible that the vortices propagating at a certain frequency f_s can excite the flat plate. Thus, in this work the case for h/D_c = 1.0 is used for the experiments.

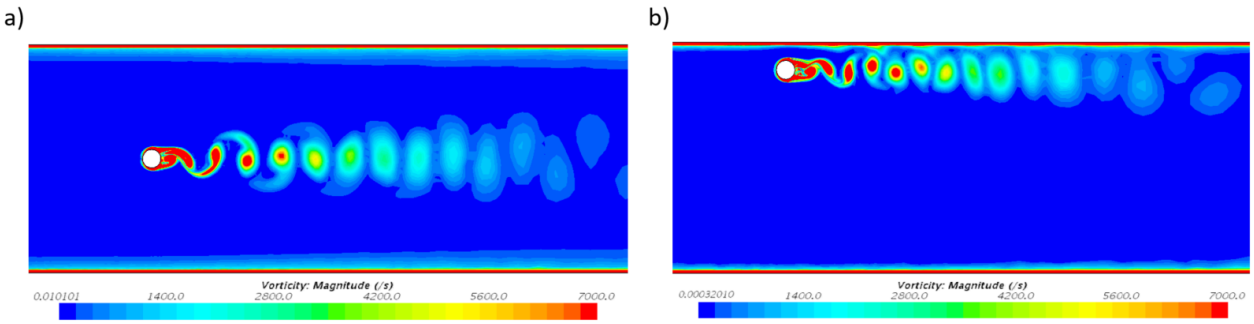

Figure 6: Vortex-shedding over a bluff cylinder of D_c = 6 mm a) h/D_c = 6.75 and b) h/D_c = 1.0.

In order to verify the vortex-shedding frequency of the generated von Karman street, the coefficient of lift spectrum for one case, namely h/D_c = 1.0, is used, as illustrated in Figure 7. In this case, the numerical vortex-shedding frequency can be predicted by the inverse of the vortex-shedding period e.g. $f_s = 1/(T_2\text{-}T_1)$, where T_1 = 0.09783 s and T_2 = 0.09936 s, which results in a vortex-shedding frequency f_s = 653.6 Hz. It is important to mention that the numerically predicted vortex-shedding frequency is slightly higher than the analytically predicted vortex-shedding frequency f_s = 600 Hz. Nevertheless, the simulations still have their value as an approximative indicator of the generated vortex-shedding and the interaction with the top plate under the considered flow conditions too.

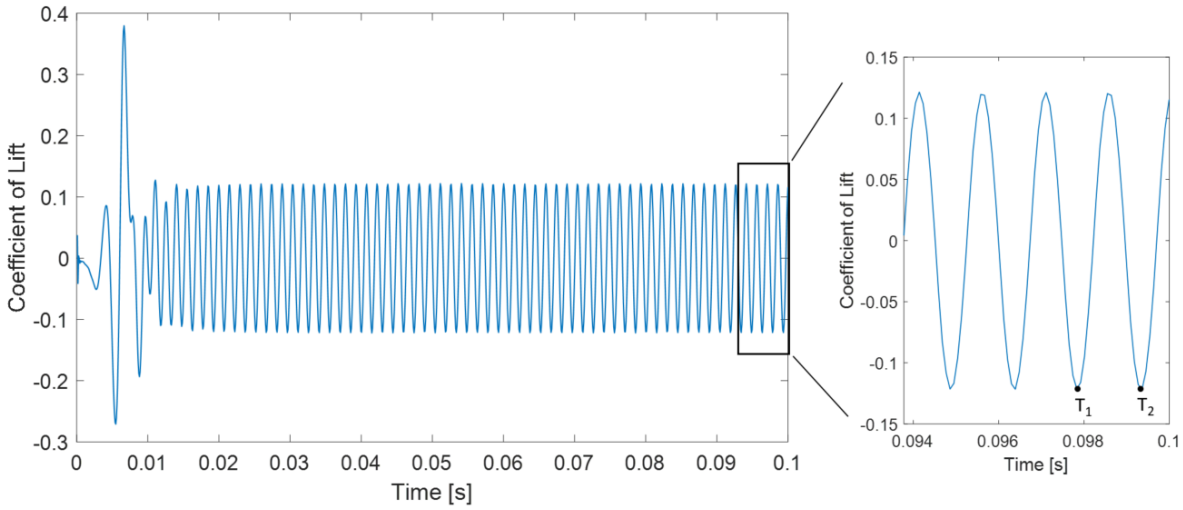

Figure 7: Coefficient of Lift versus time of the generated vortex-shedding for h/D_c = 1.0.

3 Experimental results

This section contains the experimental results regarding the vibrations of a flat plate excited by vortices formed by a bluff cylinder. The metamaterial performance in view of reducing vortex-induced vibrations is discussed as well.

3.1 Flow-induced vibrations of the flat plate

Firstly, the flat plate shown in Figure 1 is excited by turbulent fluctuating pressures due to a turbulent grazing flow of air that runs inside the aforementioned small wind tunnel at a speed U_∞ = 19 m/s. The vibrations of the bare structure due to the turbulent excitation are measured at 72 points by SLDV and the results are presented as the RMS over all points of the power spectral density spectra of the velocity. These results are used as a reference for comparison with the vortex-shedding case.

Subsequently, the flat plate is excited by a turbulent flow with a solid bluff cylinder of diameter D_c = 6 mm fixed upstream, which is designed to create a vortex-shedding with an expected frequency of f_s = 600 Hz based on the aforementioned analytical Strouhal relation, at a ratio h/D_c = 1.0, realizing the same flow conditions simulated in Section 2. Figure 8 depicts the realized bluff object and how it is placed inside the duct section. The bluff rod is glued to the system by using *Loctite*® 406™ contact adhesive.

Figure 8: Realized bluff cylinder of D_c = 6 mm placed inside the duct section.

Figure 9 illustrates the comparison between the vibrational response spectra of the bare plate excited by both a turbulent grazing flow and vortex-shedding. The two spectra are similar in shape, however, some

differences can be observed: (i) the case for a grazing flow does not contain a pronounced peak around the frequency range of interest when compared with the case without flow in Figure 2 and (ii) for the case when the bluff cylinder, designed to create a von Karman street with f_s = 600 Hz, is added to the system, the mode around the frequency range of interest and near the vortex-shedding frequency is better excited, which can indicate that the structure absorbed part of the energy coming from the vortex-shedding, as similarly evidenced by [3].

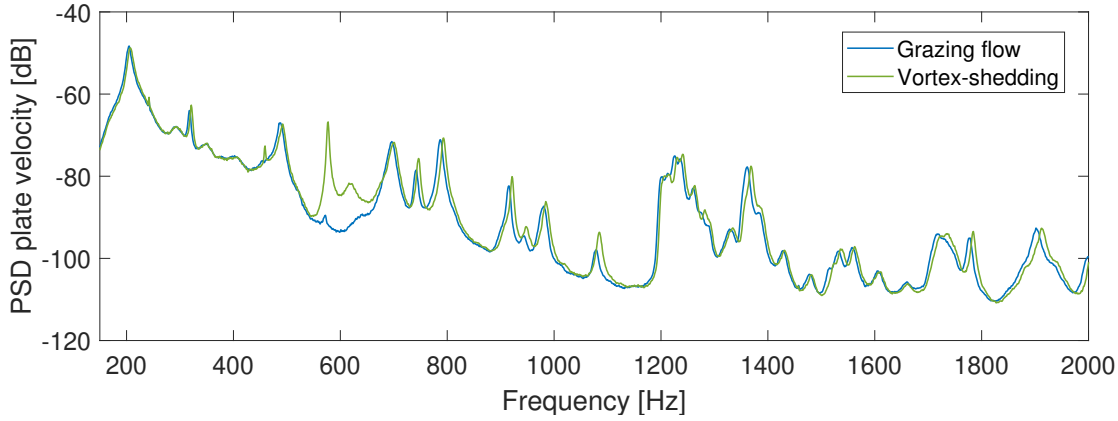

Figure 9: Comparison of PSD velocity response of the bare plate for a grazing flow and a flow with a cylinder fixed upstream for f_s = 600 Hz.

These results indicate that when vortex-shedding occurs due to the presence of a bluff object in a turbulent flow, and when its energy couples with a flexible structure, it is possible that structural resonances near the vortex-shedding frequency can be excited, which in turn could lead to a greater noise radiation. A practical problem of this phenomenon could be, for example, when the landing gear of an aircraft is deployed, it could generate a tonal noise inside the aircraft's cabin. Comparatively, in the automotive sector, when the turbulent flow finds a bluff component on the underbody of a moving car or even a luggage rack on its roof, it could generate a tonal noise inside the car's cabin. In fact, the tonal nature of the NVH behavior associated with vortex-shedding makes metamaterial solutions strong candidates given their ability to target tonal frequencies.

3.2 Metamaterial performance for vortex-induced vibrations

This present work considers two cases for the experiments regarding the vortex-shedding to be compared with the results for the bare structure: (i) the case where resonators are added on a subwavelength scale to the entire plate and (ii) the case where non-resonant structures designed with a similar mass as the resonators are periodically added to the entire plate, as shown in Figure 10. In order to validate the resonance frequency of the resonators, several samples are tested when glued to a metal block, rigidly connected to the stinger of a shaker; a similar methodology is used in [20]. The velocity at the tip of the resonator's mass is measured using SLDV. The resonators to be used in the experiments are chosen such that they have a RMS averaged resonance frequency of 600 Hz with a standard deviation of $\pm$ 0.7%.

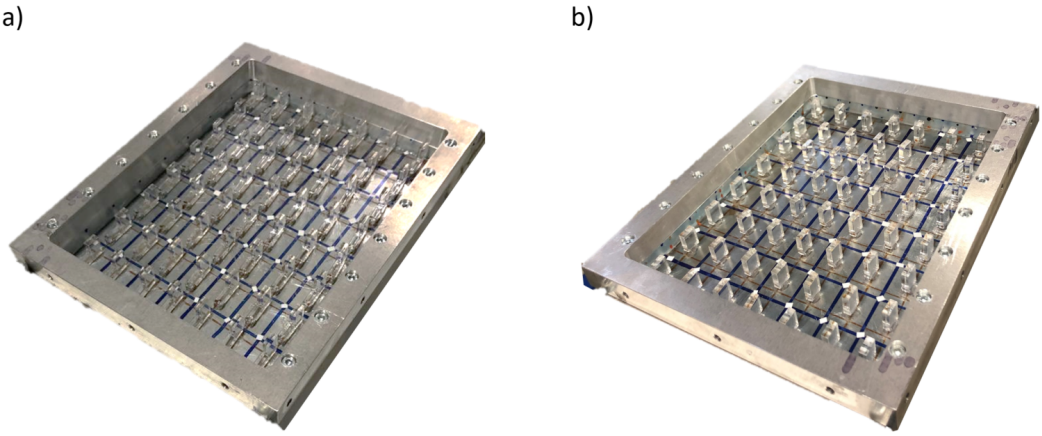

Figure 10: Illustration of the tested configurations a) resonant additions b) equivalent mass non-resonant additions.

Figure 11 compares the vortex-induced vibrational response of the flat plate with and without metamaterials for U_∞ = 19 m/s. For the metamaterial configuration, a strong dip can be found on the spectrum around the predicted stop band, whose limits are indicated by the black vertical lines. In fact, an improvement can be noticed starting from the frequency range around 400 Hz, which is explained due to the interaction between resonator and host structure and also due to the effective dynamic mass of the resonators [25]. In this case, even though the addition of the cylinder upstream caused an amplitude increase of 23 dB within the frequency range of the vortex-shedding frequency, a reduction of 36 dB is obtained by applying the designed metamaterial solution. In addition, the metamaterial solution behaves more favorably than the equivalent mass case for the test conditions. It is important to note in the spectrum that the effect of adding the resonators can also be observed at higher frequencies e.g. after the predicted stop bands, the overall amplitudes of the spectrum decreased, especially within the frequency range between 700 Hz and 1200 Hz, for which the structural modes of the bare plate can no longer be seen. This can be explained by the existence of damping in the resonant additions, which is a parameter that has a greater influence after the resonance of the resonators, suggested by the fact that the modes between 200 Hz and 400 Hz are not suppressed and only shifted due to the mass effect.

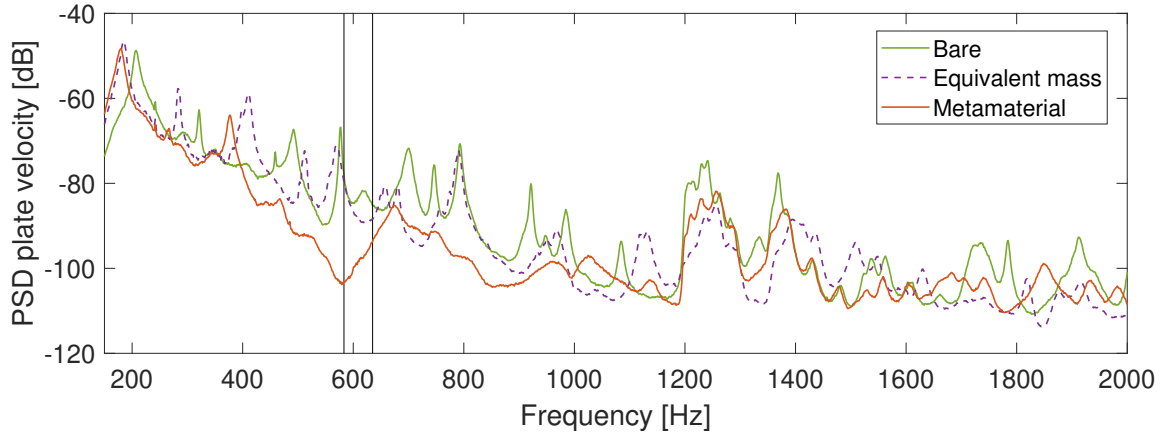

Figure 11: Experimental PSD velocity response of the flat plate with and without metamaterials for U_∞ = 19 m/s. $\mathrm{dB_{ref}}$ = 1 $(\mathrm{m/s})^2$/Hz.

4 Conclusions

This work presented an experimental investigation on the potential of using locally resonant metamaterials to suppress vortex-induced vibrations caused by a bluff object placed upstream. To this end, a flat plate excited

with a turbulent flow at a constant flow speed is considered.

Firstly, a qualitative investigation was performed by means of CFD simulations in order to have an indication of the vortex-shedding, varying the distance between the bluff body and the wall i.e. the flat plate. The study indicated that the closer the object is put to the boundary the greater is the interaction between the vortex-shedding and the wall. This assumption served as a indicator for the experiments.

The vibrations of the flat plate were experimentally measured by a Scanning Laser Doppler Vibrometer upon two excitation types: (i) a turbulent grazing flow, which served as a reference and (ii) a turbulent flow with a solid bluff cylinder of diameter D_c = 6 mm fixed upstream designed to create a vortex-shedding at f_s = 600 Hz. It has been shown that the addition of the bluff object led to an amplification of the amplitude of the structural mode near the vortex-shedding frequency when compared with the results for a grazing flow. Subsequently, a metamaterial solution is applied, targeting the frequency region where the amplification of vibrations due to the vortex-shedding was observed. Three cases are then considered, namely, the bare plate, the plate treated with sub-wavelength resonators and the plate with non-resonant additions with same mass as the designed resonators. It is shown that metamaterials provided a strong reduction of the plate's vibrations in the desired frequency range. Besides, the proposed solution is shown to outperform the equivalent mass case.

Acknowledgements

The research of F. A. Pires is funded by an Early Stage Researcher grant within the European Project SMARTANSWER Marie Curie Initial Training Network (GA 722401). The research of E. Deckers is funded by a grant from the Research Foundation – Flanders (FWO). This research was partially supported by Flanders Make, the strategic research centre for the manufacturing industry. The Research Fund KU Leuven is gratefully acknowledged for its support.

References

[1] C. Maury, P. Gardonio, and S. Elliott, "A wavenumber approach to modelling the response of a randomly excited panel, part ii: Application to aircraft panels excited by a turbulent boundary layer," *Journal of Sound and Vibration*, vol. 252, no. 1, pp. 115–139, 2002.

[2] J. Gerrard, "The mechanics of the formation region of vortices behind bluff bodies," *Journal of fluid mechanics*, vol. 25, no. 2, pp. 401–413, 1966.

[3] Y. Lau, R. So, and R. Leung, "Flow-induced vibration of elastic slender structures in a cylinder wake," *Journal of fluids and structures*, vol. 19, no. 8, pp. 1061–1083, 2004.

[4] M. M. Zdravkovich, *Flow around circular cylinders: Volume 2: Applications*. Oxford university press, 1997, vol. 2.

[5] C. Barton and J. Mixson, "Noise transmission and control for a light twin-engine aircraft," *Journal of aircraft*, vol. 18, no. 7, pp. 570–575, 1981.

[6] J. Park, L. Mongeau, and T. Siegmund, "An investigation of the flow-induced sound and vibration of viscoelastically supported rectangular plates: experiments and model verification," *Journal of sound and vibration*, vol. 275, no. 1-2, pp. 249–265, 2004.

[7] C. J. Cross and S. Fleeter, "Shunted piezoelectrics for passive control of turbomachine blading flow-induced vibrations," *Smart materials and Structures*, vol. 11, no. 2, p. 239, 2002.

[8] C. Maury, P. Gardonio, and S. J. Elliott, "Active control of the flow-induced noise transmitted through a panel," *AIAA journal*, vol. 39, no. 10, pp. 1860–1867, 2001.

[9] A. Caiazzo, N. Alujević, B. Pluymers, and W. Desmet, "Active control of turbulent boundary layer sound transmission into a vehicle interior," in *Journal of Physics: Conference Series*, vol. 744, no. 1. IOP Publishing, 2016, p. 012026.

[10] R. Camussi, *Noise sources in turbulent shear flows: fundamentals and applications*. Springer Science & Business Media, 2013, vol. 545.

[11] L. Brillouin, *Wave propagation in periodic structures: electric filters and crystal lattices*. Courier Corporation, 2003.

[12] Z. Liu, X. Zhang, Y. Mao, Y. Zhu, Z. Yang, C. T. Chan, and P. Sheng, "Locally resonant sonic materials," *science*, vol. 289, no. 5485, pp. 1734–1736, 2000.

[13] C. Goffaux, J. Sánchez-Dehesa, A. L. Yeyati, P. Lambin, A. Khelif, J. Vasseur, and B. Djafari-Rouhani, "Evidence of fano-like interference phenomena in locally resonant materials," *Physical review letters*, vol. 88, no. 22, p. 225502, 2002.

[14] P. Celli and S. Gonella, "Heterogeneity meets disorder: anomalous wave transport in telescopic metamaterials," *arXiv preprint arXiv:1703.08522*, 2017.

[15] D. Mead, "Wave propagation in continuous periodic structures: research contributions from southampton, 1964–1995," *Journal of sound and vibration*, vol. 190, no. 3, pp. 495–524, 1996.

[16] M. I. Hussein, "Reduced bloch mode expansion for periodic media band structure calculations," *Proceedings of the Royal Society A: Mathematical, Physical and Engineering Sciences*, vol. 465, no. 2109, pp. 2825–2848, 2009.

[17] A. Dewan, *Tackling turbulent flows in engineering*. Springer Science & Business Media, 2010.

[18] C. C. Claeys, K. Vergote, P. Sas, and W. Desmet, "On the potential of tuned resonators to obtain low-frequency vibrational stop bands in periodic panels," *Journal of Sound and Vibration*, vol. 332, no. 6, pp. 1418–1436, 2013.

[19] F. Bloch, "Über die quantenmechanik der elektronen in kristallgittern," *Zeitschrift für physik*, vol. 52, no. 7-8, pp. 555–600, 1929.

[20] C. Claeys, N. G. R. de Melo Filho, L. Van Belle, E. Deckers, and W. Desmet, "Design and validation of metamaterials for multiple structural stop bands in waveguides," *Extreme Mechanics Letters*, vol. 12, pp. 7–22, 2017.

[21] F. Alves Pires, C. Claeys, E. Deckers, and W. Desmet, "Influence of the footprint of resonant additions on the stop band behaviour of 1d locally resonant metamaterials," in *INTER-NOISE and NOISE-CON Congress and Conference Proceedings*, vol. 259, no. 7. Institute of Noise Control Engineering, 2019, pp. 2081–2091.

[22] F. Alves Pires, L. Sangiuliano, H. Denayer, E. Deckers, C. Claeys, and W. Desmet, "Suppression of flow-induced noise and vibrations by locally resonant metamaterials," in *AIAA AVIATION 2020 FORUM*, 2020, p. 2586.

[23] T. Nakamura, S. Kaneko, F. Inada, M. Kato, K. Ishihara, T. Nishihara, N. W. Mureithi, and M. A. Langthjem, *Flow-induced vibrations: classifications and lessons from practical experiences*. Butterworth-Heinemann, 2013.

[24] T. Nishino, G. Roberts, and X. Zhang, "Unsteady rans and detached-eddy simulations of flow around a circular cylinder in ground effect," *Journal of Fluids and Structures*, vol. 24, no. 1, pp. 18–33, 2008.

[25] N. de Melo Filho, L. Van Belle, C. Claeys, E. Deckers, and W. Desmet, "Dynamic mass based sound transmission loss prediction of vibro-acoustic metamaterial double panels applied to the mass-air-mass resonance," *Journal of Sound and Vibration*, vol. 442, pp. 28–44, 2019.